Journal of Materials Science: Materials in Electronics (2019) 30:1998–2005
https://doi.org/10.1007/s10854-018-0471-5

Manganese oxide nanoparticles electrodeposited on graphenized pencil lead electrode as a sensitive miniaturized pH sensor

Rahim Mohammad-Rezaei[1] · Sahand Soroodian[1] · Ghadir Esmaeili[1]

Received: 20 October 2018 / Accepted: 27 November 2018 / Published online: 30 November 2018

Abstract
pH monitoring in micro volume samples is required for environmental and clinical analysis. Low cost, miniaturized and stable metal oxide based pH sensors could be a suitable alternative to glass electrodes. In this study, a sensitive potentiometric solid state pH sensor based on manganese oxide nanoparticles electrodeposited on graphenized pencil lead electrode (MnO_2/GPLE) was reported. The prepared MnO_2/GPLE was carefully characterized by SEM, XRD and electrochemical techniques. To miniaturize the prepared pH sensor, a stainless steel 304 needle was used as a reference electrode. Selectivity, response time, stability and reproducibility of the miniaturized pH sensor were studied and compared with conventional glass pH electrode. According to experimental results, a near-Nernstian slope of − 57.051 mV/pH and linearity over the pH range of 1.5–12.5 were obtained for the developed MnO_2/GPLE pH sensor. The prepared sensor represented high ion selectivity to mono-valence and multi-valence ions with $-\log K^{Pot}_{A,B}$ values around 6.49. A fast response time of 20 s in acidic medium and 60 s in alkaline medium, long-term stability and reproducibility in 2 months, the simplicity of fabrication, low cost and accuracy makes this sensor as a suitable choice for rapid pH recording in micro volume samples. The MnO_2/GPLE pH sensor was successfully used for the pH monitoring of human tear, human blood, saliva, apple juice, lemon juice, milk, and vinegar samples with satisfactory results.

1 Introduction

pH value of aqueous solutions is one of the most significant parameters in the industry, agriculture, pharmaceutical, human health, environmental control and biological systems. As the measurement of pH is required daily, there is an emerging necessity for rapid, non-degradable, portable and cost-effective methods for this purpose. Up to now, glass pH electrode has been in use as a commercial electrode for pH assessments [1]. Acceptance of glass pH electrode is due to its selectivity, repeatability, and ease of use. However, some drawbacks such as high expense, temperature instability, need for the internal standard solution, upright positioning (applicable only in a vertical position) and inaccuracies in highly acidic and alkali media have restricted its utilization in certain circumstances. Also, determination of pH value in low volumes is necessitating the need for miniaturization of pH electrodes.

For overcoming these restrictions, various solid state non-glass pH electrodes have been developed [2–5]. Because of mechanical stability and low interference to metal ions, various metal oxides based solid state pH sensors such as platinum, titanium, ruthenium, iridium, lead, zirconium, tin, cobalt, and tungsten oxide have been reported [6–14].

Metal oxides could be deposited on various surfaces for the fabrication of metal oxide pH electrodes. Graphene is a honey comb and single layer of carbon with high electric conductivity and good adsorption potential which could be utilized as substrate for the assembly of electrochemical devices [15–17]. During the last decade various electrochemical sensors and biosensors based on graphene, graphene oxide, reduced graphene oxide and graphene quantum dots were reported. Due to the problematic multi-step synthesis of graphene based materials and purification process, the need for a fast and cost-effective method for graphene synthesis has highlighted. Electrochemical exfoliation of graphite is an efficient route for creating desired graphene nano-sheets in one single step. This method has

✉ Rahim Mohammad-Rezaei
r.mohammadrezaei@azaruniv.ac.ir;
r.mohammadrezaei@ymail.com

[1] Electrochemistry Research Lab, Faculty of Basic Sciences, Azarbaijan Shahid Madani University, Tabriz, Iran

been successfully used for the developing of electrochemical sensors, adsorbents and storage devices [18–21].

Pencil Lead electrode (PLE) is a cheap, easily affordable electrically conductive and mechanically stable electrode which could be easily exploited for electrochemical purposes. Recently PLE has been reported to be exfoliated to graphene nano-sheets by applying a direct electric potential to the electrode surface [22–24]. Due to remarkable conductivity, high porosity, notable surface area and outstanding electrode transfer rate, graphenized pencil lead electrode (GPLE) could be a suitable electrode candidate for electrodeposition of various nanoparticles such as metal oxides.

In this study, manganese oxide nanoparticles have been deposited electrochemically on the surface of GPLE for construction of a novel potentiometric pH sensor. To miniaturize the pH sensor, a stainless steel hollow needle of a conventional injection syringe was used as a reference electrode [25] and a mechanical pencil lead was employed to perform as a graphite based working electrode. The experimental results obtained for the developed pH sensor were compared with the conventional glass pH electrode which yielded satisfactory results. The miniaturized solid state MnO_2/GPLE has a suitable potential for sensitive and selective monitoring of pH routinely with low cost in micro volume samples.

2 Experimental

2.1 Chemicals

Manganese sulfate ($MnSO_4 \cdot H_2O$) was from Sigma-Aldrich (St. Louis, MO, USA) and stock solution with a concentration of 0.02 was prepared in double distilled water. The pencil graphite rod (HB type) was from Rotring Co. LTD, Germany (R 505210N) with a diameter of 0.5 mm. Hollow stainless needle was purchased from a local provider and maintained in 2 M HCl (as treatment solution) for 6 h. Phosphate buffer solutions (PBS) with different pHs were prepared at an initial concentration of 0.1 M using NaH_2PO_4 and pH was adjusted by HCl and NaOH solutions.

2.2 Apparatus

Cyclic voltammetry (CV) was carried out by an AUTOLAB PGSTAT-204 (potentiostat/galvanostat) with three electrode system; A platinum wire and saturated calomel as auxiliary and reference electrodes respectively and MnO_2 nanoparticles modified graphenized pencil lead electrode (MnO_2/GPLE) as the working electrode. Potentiometry (pH measurement) studies were carried out using a Metrohm pH meter (827 pH lab). The utilized dual-electrode system in potentiometry studies was composed of a stainless steel needle as the reference electrode and fabricated MnO_2/GPLE as the indicator electrode. Scanning electron microscopy (SEM) images and X-ray diffraction were obtained using a Phenom ProX scanning electron microscope (Hitachi, Tokyo, Japan) and a Bruker AXF (D8 Advance) X-ray powder diffractometer respectively. A conventional AC/DC power supply was used for electrochemical exfoliation of pencil lead electrodes.

2.3 Preparation of graphenized pencil lead electrode (GPLE)

In this study, the pencil lead was electrochemically exfoliated [22, 24] to prepare the GPLE as follows: Firstly, the provided pencil leads were polished using polishing papers and after communicating the electrical contact with a copper wire, the resulted electrode was wrapped in Teflon stripes. Two brown PLE as anode and cathode was rinsed with doubly distilled water and vertically immersed in 1 M sulfuric acid solution for exfoliation process. The electrochemical exfoliation was carried out by applying an optimized potential with the alternating bias between + 8 and − 8 V for five cycles (each cycle consisting of 1 s). The obtained anode electrode with the dark black surface was called graphenized pencil lead electrode (GPLE) which finally was washed with double distilled water and stored in room temperature until further use.

2.4 Fabrication of MnO_2 nanoparticles modified GPLE (MnO_2/GPLE)

For fabrication of MnO_2/GPLE, the prepared GPLE were rinsed and dipped into 1 mM Mn^{2+} solution containing 0.05 M PBS solution (pH 7). Then continuous CVs were conducted under constant stirring (200 rpm) for 15 cycles over the potential range of − 1.0 to 1.6 V at a sweep rate of 100 mV s^{-1}. Figure 1 shows the CVs of the GPLE during the electrodeposition of MnO_2 nanoparticles. It is visible that by cycling the potential, the peak currents gradually grow and reach to a maximum value after 15 nearly cycles. The growing of peak currents and a slight shift of peak potentials is an indication of successful electrodeposition and formation of a thin layer of manganese oxide nanoparticles on the GPLE [26].

Two apparent anodic peaks at 0.56 V and 1.21 V and also cathodic peaks at 0.83 V and − 0.42 V are related to the quasi-reversible redox reactions between the Mn^{2+}/Mn^{3+} and Mn^{3+}/Mn^{4+} which could be described with following equations respectively [27]:

$$Mn^{2+} + 2\,H_2O \rightarrow MnOOH + 3\,H^+ + e^- \quad (1)$$

$$MnOOH \rightarrow MnO_2 + H^+ + e^- \quad (2)$$

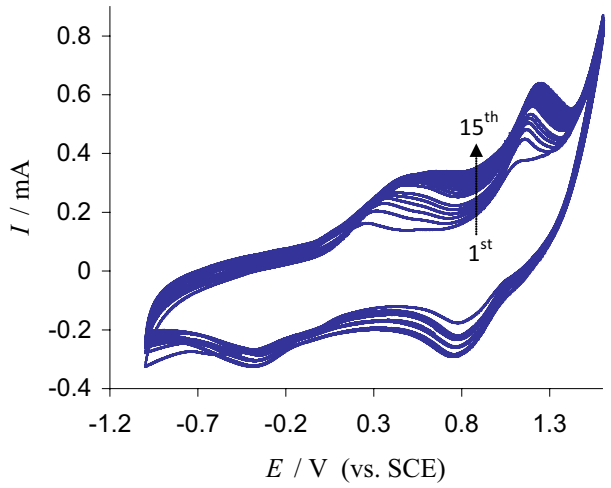

Fig. 1 Continuous CVs of the GPLE during the electrodeposition of MnO_2 nanoparticles at sweep rate is 100 mV s^{-1}; Solution containing 1 mM Mn^{2+} and 0.05 M phosphate buffer solution (pH 7)

Also, deposition of MnO_2 on GPLE could be properly described with an ECE equation:

$$Mn^{2+} \xrightarrow{E} Mn^{3+} + e^- \quad (3)$$

$$Mn^{3+} + 2H_2O \xrightarrow{C} MnOOH + 3H^+ \quad (4)$$

$$MnOOH \xrightarrow{E} MnO_2 + H^+ + e^- \quad (5)$$

Also, electrodeposition of Manganese oxide on PLE (MnO_2/PLE) in identical conditions represents similar but very smaller peak currents and pretty same peak potentials (not shown). The heightened peak currents in MnO_2/GPLE may be originating from enhanced conductivity, improved electron transfer property and high surface area of GPLE which properly coated with MnO_2 nanoparticles. Finally, the prepared MnO_2/GPLE was rinsed with distilled water and dried with N_2 stream and stored until the electrochemical studies. To miniaturize the MnO_2/GPLE pH sensor setup, the prepared electrode was joint with a stainless steel needle as the reference electrode. The photo image/scheme of the assembled MnO_2/GPLE pH sensor is presented in Scheme 1.

3 Results and discussion

3.1 Characterization of MnO_2/GPLE

SEM image of the GPLE with magnification the of 50,000 was shown in Fig. 2a. As can be seen, graphite is well exfoliated and a three-dimensional layered structure of graphene

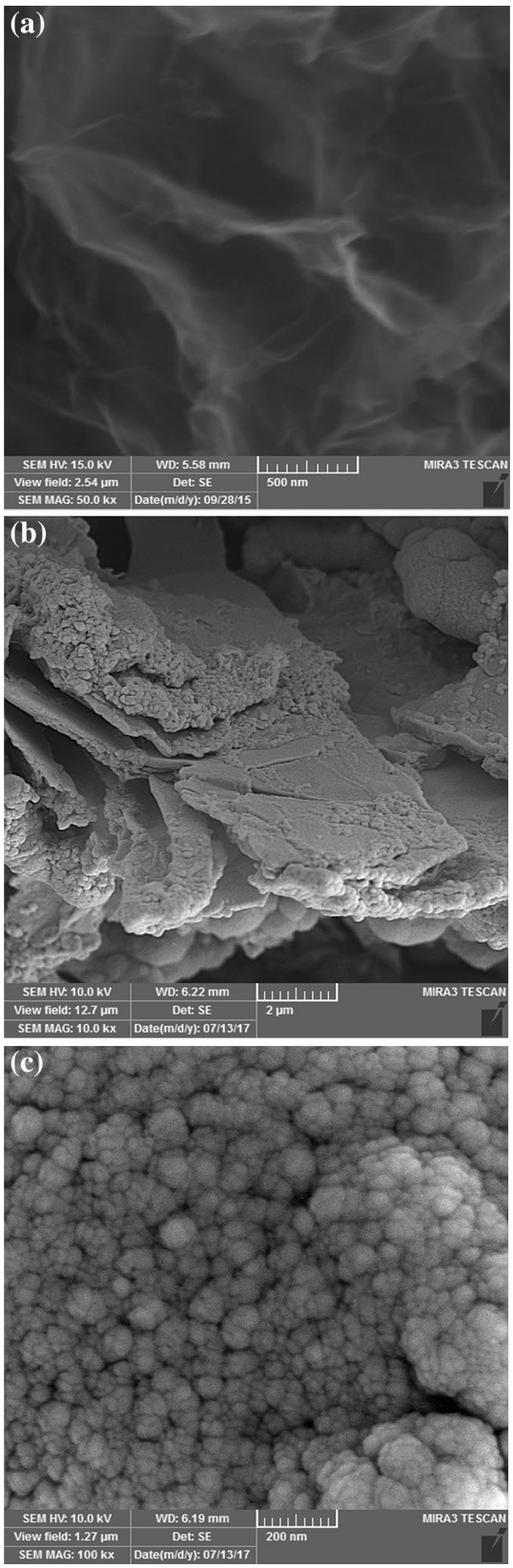

Fig. 2 SEM images of GPLE (**a**) and MnO_2/GPLE (**b, c**) with magnifications of 10,000 and 100,000 respectively

on the surface of the GPLE was constructed. SEM images of the MnO_2/GPLE with magnifications of 10,000 and 100,000 were shown in Fig. 2b, c respectively. According to these images, a multi-pore and scaly network of the MnO_2/GPLE with granular and nano-porous morphology was formed. The images show that MnO_2 nanoparticles are properly trapped in the network of the GPLE. This study approves the appropriateness of the GPLE for the deposition of solid state transition metal oxides and assembly of electrochemical devices. Also, a layered structure of GPLE could be helpful for mass transfer and stabilization of electroactive species in modified electrodes.

To acquire excess information about the electrodeposited of MnO_2 on the GPLE, XRD pattern of the electrodes were studied. Figure 3 shows the XRD patterns of PLE (A), GPLE (B) and MnO_2/GPLE (C). The distinctive peak at $2\theta = 26.2°$ for PLE is attributed to the (002) plane of the hexagonal graphite structure. The peak at (002) is broadened after the graphenization of PLE proving the interlayer increase in the case of GPLE [28]. XRD pattern of MnO_2/GPLE contains broad peaks at $2\theta = 28.8°$, 36.8°, 42.6° and 50.1° corresponding to α-MnO_2 [29, 30]. Also, the XRD pattern of the MnO_2/GPLE shows the broad (002) peak of graphene implying that the MnO_2 nanoparticles are well integrated into the conductive GPLE network. According to XRD analysis, the nucleation and growth of MnO_2 nanoparticles on GPLE as a carrier could be concluded.

3.2 Electrochemical behavior of MnO_2/GPLE

Sweeping the potential between the − 1.0 and 1.5 V in supporting electrolytes such as PBS (0.01 M, pH 7) and KOH (pH 12) did not show any obvious decrease in the redox peak currents of MnO_2/GPLE which confirm the electrochemical stability of the prepared electrode. Figure 4 shows the CV of the MnO_2/GPLE in 0.01 M KOH solution after 30 continuous cycles. The quasi-reversible anodic and cathodic peaks could be associated to the surface-confined electrochemical

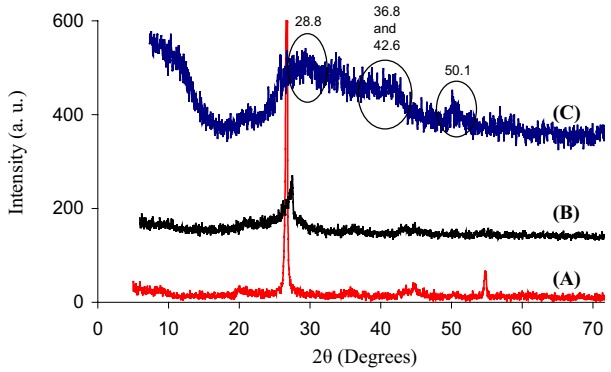

Fig. 3 XRD patterns of PLE (a), GPLE (b) and MnO_2/GPLE (c)

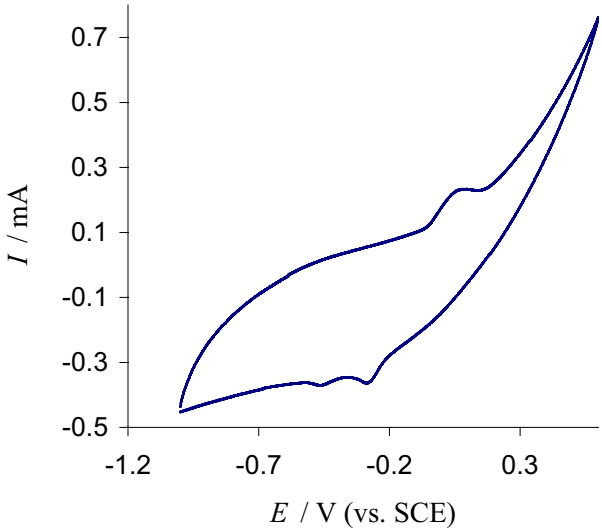

Fig. 4 CV of the MnO_2/GPLE in 0.01 M KOH at the scan rate of 100 mV s^{-1}

reactions between the MnOOH and MnO_2 which has been deposited on the electrode surface. According to this study, after 30 continuous cycles, the decrease of peak currents was only 2.1% proving the high chemical stability of the fabricated electrode.

3.3 Potentiometric response and pH sensing of the MnO_2/GPLE

pH sensing of metal oxides involves a potentiometric response which originates from the equilibrium between the two solid phases of the metal oxide and/or the introduce of species into the metal oxide structure. The equation which describes the pH sensing function of MnO_2/GPLE could be represented as Eq. 6 which originated from the redox reaction and proton exchange between the MnO_2 and MnOOH. According to this theory, Open Circuit Potential (OCP) or equilibrium potential ($E_{MnO_2/MnOOH}$) could be expressed by Nernst equation [31]:

$$E_{\frac{MnO_2}{MnOOH}} \text{ vs. SHE} = E^{\circ}_{\frac{MnO_2}{MnOOH}} \text{ vs. SHE} + \frac{RT}{nF} ln \frac{a_{MnO_2}\, a_{H^+}}{a_{MnOOH}} \quad (6)$$

where E and E° are the measured and standard potential respectively, R is the gas constant (8.314 J K^{-1} mol^{-1}), F is the Faraday constant (96487.3415 C mol^{-1}), and T is the absolute temperature (K).

By considering a constant value for and on the electrode surface, and also stainless steel needle as the reference electrode, Eq. 6 could be written as:

$$E = \text{constant} - 0.05916\ \text{pH} \quad (7)$$

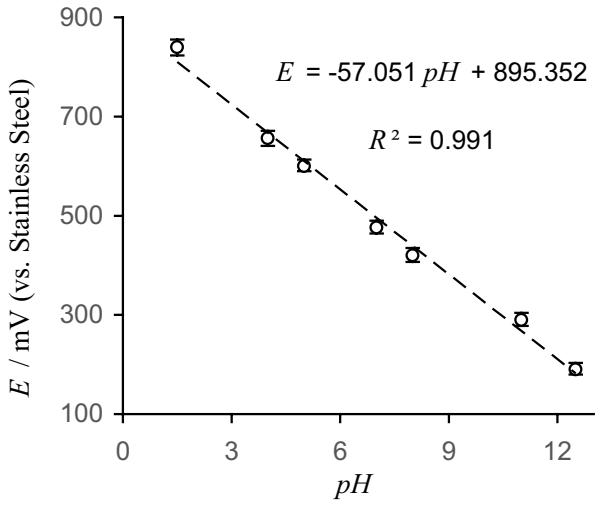

Fig. 5 Relation between the OCP (vs. stainless steel) and pH value measured at MnO_2/GPLE

According to this equation, the plot of measured potential in relation to pH values results a straight line with a slope of −59.16 mV/pH (25 °C). To evaluate the pH sensing function of fabricated MnO_2/GPLE, potentiometry method was conducted in numerous solutions with various predefined pHs (Fig. 5). According to this study, the relation between the obtained potentials with respected pHs, is linear (R^2 = 0.991) over the suitable pH range with the slope of −57.051 which is close to the theoretical value (Eq. 7).

Reproducibility of preparation procedure of the MnO_2/GPLE should be considered for the commercialization. For this purpose, potentiometric response and sensitivity of the five repetitively and independently prepared MnO_2/GPLE were put to the test and results were presented in Fig. 6a. The RSD values for slopes and intercepts of the results obtained electrodes were calculated to be 3.23% and 2.26% respectively proving appropriate reproducibility during the preparation procedure.

To propose an efficient pH sensor for practical uses, response time and sudden changes in pH values must be assessed. The response time of MnO_2/GPLE for quick pH change was studied at hydrodynamic conditions in two different pH solutions in sequence and sudden changes (pH 12.5 and 1.5). The step-change response of the MnO_2/GPLE is shown in Fig. 6b representing good step repeatability and fast response in both directions. As shown in Fig. 6b the step change of pH from acidic to alkali media was very fast which the time needed for 90% of the response (t_{90}) was about 20 s. On the contrary, the step from basic to acidic media was relatively slow (t_{90} = 60 s) which shows a smooth curve resulted by the gradual increase in measured potential. This phenomenon may be due to the slower nature of interactions between electrode surface and solution in the

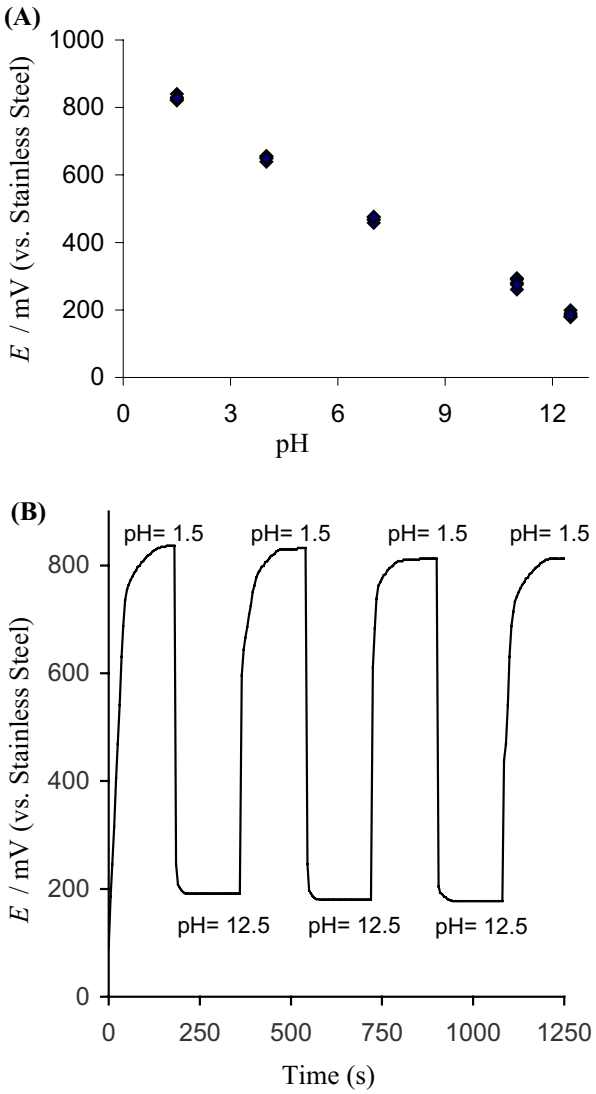

Fig. 6 Relation between the pH value and potentiometric response of five different c (**a**) and potentiometric response of MnO_2/GPLE to sudden pH change (**b**)

basic environment. As memory effect could cause a delay in potentiometry response of pH electrodes [32]. The t_{90} values of the developed pH sensor in both directions were less than 1 min in both cases suggesting suitable response time of the MnO_2/GPLE for practical applications in different samples. When the electrode potential reached to the steady state at determined pH, a little alteration in the electrode potential was seen after 2 h (> 3.6%) emphasizing the effectiveness of the developed solid state pH sensor.

Sensitivity, dynamic pH range and response time of the developed MnO_2/GPLE pH sensor were compared with some other non-glass pH sensors, and the results were summarized in Table 1. As can be seen, the dynamic pH range and response time was improved and/or comparable with respect to similar metal oxides pH sensors [3, 33–36].

Table 1 Analytical data of MnO_2/GPLE and some recently reported solid state pH sensors

Electrode material	Slope (mV/pH)	Response time (s)	Dynamic pH range	References
Conductive polymer/AuZn Oxide	59.2	–	2–13	[3]
Reduced graphene oxide	40.19	–	4–10	[33]
MnO_2-montmorillonite	55.01	120	1.6–12.5	[34]
Ruthenium dioxide	59.15	600	2–10	[35]
Tantalum pentoxide	24.18	–	1–13	[36]
Miniaturized MnO_2/GPLE	57.05	60	1.5–12	This work

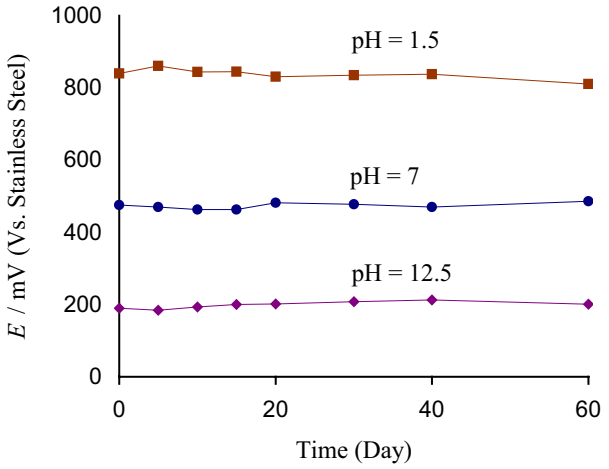

Fig. 7 Long-term stability of the MnO_2/GPLE in acidic, natural and basic media

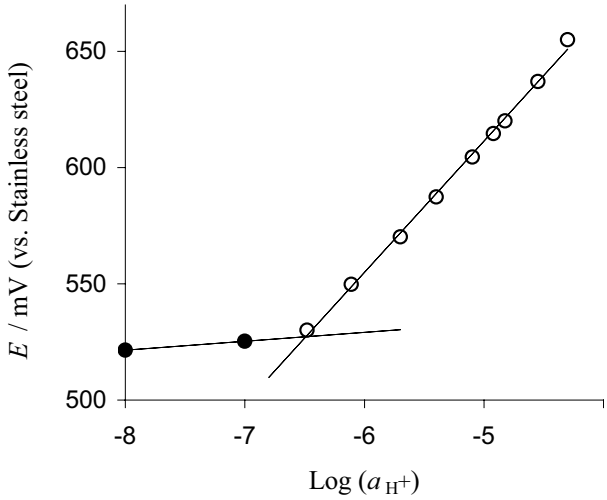

Fig. 8 Selectivity coefficient determination of the MnO_2/GPLEfor the interfering cation K^+ (fixed concentration of 0.01 M) with respect to the principal ion H^+

3.4 Stability of the MnO_2/GPLE

The long-term stability of MnO_2/GPLE in acidic, neutral and basic media was explored for a period of 60-day (Fig. 7). According to this study, the developed solid state pH sensors represented high stability during the long-term usage. Also, when the prepared electrodes were kept in the air or partially used to test for a period of 2 months, the response and sensitivity become nearly unchanged and just 7.6 mV drift in slope was observed for three examined electrodes. Long-term stability of the MnO_2/GPLE could be mainly related to the appropriate attachment of MnO_2 nanoparticles into the porous structure of GPLE. Considering low cost, easy preparation procedure and high stability of the developed sensor, the proposed sensor is a fine candidate for routine pH analysis in daily experiments.

3.5 Selectivity

Metallic cations particularly alkali-cations may interfere in the response of pH sensors and reduce the selectivity of electrodes. According to the fixed interference method, the effect of some interfering cations such as Na^+, K^+, Li^+, Mg^{2+} and Ca^{2+}on the potentiometric response of the MnO_2/GPLE was evaluated. In this study, the emf value of the MnO_2/GPLE versus stainless steel reference electrode was measured in the solutions with constant activity (10^{-2} M) of interfering cation, a_M, and increasing the activity of the H^+ ion. Figure 8 shows the plot of obtained emf values versus the log a_{H+} in the presence of 0.01 M K^+. The meeting point of the linear portions of this plot indicates the value of a_{H+} which could be used for the calculation of according to Nikolsky–Eisenman equation [37]:

$$E = \text{Constant} + \frac{2.303\ RT}{z_A F} \times \log\left[a_A + K^{\text{Pot}}_{A,B}\, a_B^{Z_A/Z_B} + K^{\text{Pot}}_{A,C}\, a_C^{Z_A/Z_C} + \ldots\right] \quad (8)$$

$$K^{\text{Pot}}_{A,B} = \frac{a_A}{a_B^{z_{A/Z_B}}} \quad (9)$$

where $K^{\text{Pot}}_{A,B}$ is the potentiometric selectivity coefficient for ion B with the activity of a_B with respect to the ion A with

the activity of a_A. According to experimental results values for Na^+, K^+, Li^+, Mg^{2+} and Ca^{2+} were calculated to be 4.46, 4.39,4.48, 4.53 and 4.49 respectively. Also the interfering of some anions on the response of MnO_2/GPLE pH sensor was investigated (Table 2). As can be seen, the pH response of the MnO_2/GPLE has not changed remarkably in the presence of examined anions proving high selectivity of the developed solid state pH sensor.

3.6 Analytical applications and pH measurements in real samples

To evaluate the performance of the MnO_2/GPLE pH sensor, the titration of hydrochloric acid as a strong acid (0.01 M) by standard potassium hydroxide solution (0.01 M) were carried out (Fig. 9), and the responses were compared with a glass pH electrode in similar conditions. As it can be seen, the developed pH sensor and standard glass pH electrode show appropriately similar responses in acid-base titration and the end-points are close together, hence proving the practicability of the sensor in the acid-base titration.

To evaluate the efficacy of the developed miniaturized pH sensor in complex matrixes, and also in micro volume, pH values of some real samples such as vinegar, milk, apple juice, lemon Juice, saliva, human blood and human tear were examined and compared with the pH values determined with a commercial glass pH electrode. The good agreement obtained with the two electrodes (Table 3) proves the potential of the MnO_2/GPLE for the real test applications and routine pH analysis. According to the t-test analysis, there is no systematical at the confidence level of 95% between the developed pH sensor and commercial glass pH electrode.

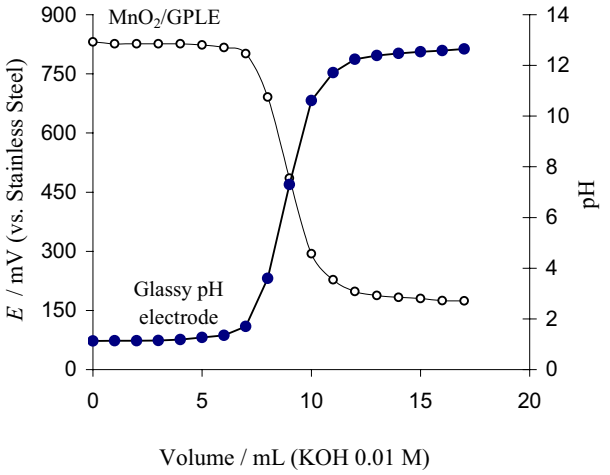

Fig. 9 Titration of HCl (0.01 M) with NaOH (0.01 M) using glass pH electrode and MnO_2/GPLE pH sensor (B)

Table 3 pH of some real samples measured by GPLE/MnO_2 and compared with glassy pH electrode

Sample	pH value[a] determined with GPLE/MnO_2	pH value[a] determined with glassy pH electrode
Human tear	6.71	Unable
Human blood	7.31	Unable
Saliva	6.91	Unable
Lemon juice	2.35	2.41
Apple juice	3.29	3.28
Cow milk	6.51	6.55
Vinegar	3.65	2.96

[a]Average of three repeat

4 Conclusion

In this study, the preparation and pH response of a new miniaturized pH sensor based on MnO_2/GPLE was reported. The developed solid state pH sensor responds to pH values between 1.5 and 12.5 with near Nernstian slope of −57.051 mV/pH. The developed MnO_2/GPLE pH sensor represents high selectivity, small response time, good stability and reproducibility in comparison with another solid state pH sensor. The simplicity of fabrication, low cost and accuracy make this sensor as a suitable choice for rapid pH recording in micro volume samples.

Table 2 Relative error (%) on the potentiometric response of the MnO_2/GPLE caused by interfering anions

Interfering species	Relative error (%)
NO_3^-	3.14
Cl^-	2.68
Br^-	2.87
I^-	3.12
SO_4^{2-}	2.45
CH_3COO^-	2.36
CO_3^{2-}	2.14
PO_4^{3-}	2.69

Acknowledgements The authors gratefully acknowledge the Research Council of Azarbaijan Shahid Madani University for financial support.

References

1. M. Dole, J. Chem. Educ. **57**, 134 (1980)
2. C. Hegarty, S. Kirkwood, M.F. Cardosi, C.L. Lawrence, C.M. Taylor, R.B. Smith et al., Microchem. J. **139**, 210 (2018)
3. D.-M. Kim, S.J. Cho, C.-H. Cho, K.B. Kim, M.-Y. Kim, Y.-B. Shim, Biosens. Bioelectron. **79**, 165 (2016)
4. M. Glanc-Gostkiewicz, M. Sophocleous, J.K. Atkinson, E. Garcia-Breijo, Sens. Actuators A **202**, 2 (2013)

5. B.C. Thompson, O. Winther-Jensen, B. Winther-Jensen, D.R. MacFarlane, Anal. Chem. **85**, 3521 (2013)
6. W. Lonsdale, M. Wajrak, K. Alameh, Talanta **180**, 277 (2018)
7. S.A.M. Marzouk, Anal. Chem. **75**, 1258 (2003)
8. T. Hashimoto, M. Miwa, H. Nasu, A. Ishihara, Y. Nishio, Electrochim. Acta **220**, 699 (2016)
9. B. Xu, W.-D. Zhang, Electrochim. Acta **55**, 2859 (2010)
10. L. Qingwen, L. Guoan, S. Youqin, Anal. Chim. Acta **409**, 137 (2000)
11. L.A. Pocrifka, C. Gonçalves, P. Grossi, P.C. Colpa, E.C. Pereira, Sens. Actuators B **113**, 1012 (2006)
12. A. Eftekhari, Sens. Actuators B **88**, 234 (2003)
13. R.H. Zhang, X.T. Zhang, S.M. Hu, Anal. Chem. **80**, 2982 (2008)
14. L. Santos, J.P. Neto, A. Crespo, D. Nunes, N. Costa, I.M. Fonseca et al., ACS Appl. Mater. Interfaces **6**, 12226 (2014)
15. N. Baig, T.A. Saleh, Microchim. Acta **185**, 283 (2018)
16. X.-C. Dong, H. Xu, X.-W. Wang, Y.-X. Huang, M.B. Chan-Park, H. Zhang et al., ACS Nano **6**, 3206 (2012)
17. C. Xu, B. Xu, Y. Gu, Z. Xiong, J. Sun, X.S. Zhao, Energy Environ. Sci. **6**, 1388 (2013)
18. Y. Zhang, Y. Xu, J. Zhu, L. Li, X. Du, X. Sun, Carbon **127**, 392 (2018)
19. R. Singh, C.C. Tripathi, Mater. Today Proc. **5**, 1125 (2018)
20. P.C. Shi, J.P. Guo, X. Liang, S. Cheng, H. Zheng, Y. Wang et al., Carbon **126**, 507 (2018)
21. H. Wang, C. Wei, K. Zhu, Y. Zhang, C. Gong, J. Guo et al., ACS Appl. Mater. Interfaces **9**, 34456 (2017)
22. Q. Liu, M. Cheng, Y. Long, M. Yu, T. Wang, G. Jiang, J. Chromatogr. A **1325**, 1 (2014)
23. K. Chen, D. Xue, S. Komarneni, J. Colloid Interface Sci. **487**, 156 (2017)
24. R. Mohammad-Rezaei, S. Soroodian, Sens. Lett. **15**, 729 (2017)
25. J.P. Wilburn, M. Ciobanu, N.I. Buss, D.R. Franceschetti, D.A. Lowy, Anal. Chim. Acta **511**, 83 (2004)
26. H. Razmi, R. Mohammad-Rezaei, Electrochim. Acta **56**, 7220 (2011)
27. N. Cherchour, C. Deslouis, B. Messaoudi, A. Pailleret, Electrochim. Acta **56**, 9746 (2011)
28. F.T. Johra, J.-W. Lee, W.-G. Jung, J. Ind. Eng. Chem. **20**, 2883 (2014)
29. T. Cetinkaya, M. Tokur, S. Ozcan, M. Uysal, H. Akbulut, Int. J. Hydrog. Energy **41**, 6945 (2016)
30. X. Wang, Y. Li, Chem. Commun. **7**, 764 (2002)
31. H. Razmi, H. Heidari, E. Habibi, J. Solid State Electrochem. **12**, 1579 (2008)
32. W.E. Morf, E. Pretsch, N.F. de Rooij, J. Electroanal. Chem. **633**, 137 (2009)
33. P. Salvo, N. Calisi, B. Melai, B. Cortigiani, M. Mannini, A. Caneschi et al., Biosens. Bioelectron. **91**, 870 (2017)
34. L. Telli, B. Brahimi, A. Hammouche, Solid State Ionics **128**, 255 (2000)
35. J.A. Mihell, J.K. Atkinson, Sens. Actuators B **48**, 505 (1998)
36. Y.-C. Wu, S.-J. Wu, C.-H. Lin, Microsyst. Technol. **23**, 293 (2017)
37. W. Prissanaroon-Ouajai, P.J. Pigram, R. Jones, A. Sirivat, Sens. Actuators B **135**, 366 (2008)